Computers and Chemical Engineering 93 (2016) 13–24

Contents lists available at ScienceDirect

Computers and Chemical Engineering

journal homepage: www.elsevier.com/locate/compchemeng

Nonlinear control of the dissolved oxygen concentration integrated with a biomass estimator for production of *Bacillus thuringiensis* δ-endotoxins

Santiago Rómoli [a,*], Adriana Natacha Amicarelli [b], Oscar Alberto Ortiz [a], Gustavo Juan Eduardo Scaglia [a], Fernando di Sciascio [b]

[a] Instituto de Ingeniería Química, Universidad Nacional de San Juan, Av. Lib. San Martín Oeste 1109, San Juan, Argentina
[b] Instituto de Automática, Universidad Nacional de San Juan, Av. Lib. San Martín Oeste 1109, San Juan, Argentina

ARTICLE INFO

Article history:
Received 28 September 2015
Received in revised form 5 May 2016
Accepted 27 May 2016
Available online 4 June 2016

Keywords:
δ-Endotoxins production dissolved oxygen control
Nonlinear dynamic inversion
Batch bioprocess
Bacillus thuringiensis

ABSTRACT

Bacillus thuringiensis is a microorganism that allows the biosynthesis of δ-endotoxins with toxic properties against some insect larvae, being often used for the production of biological insecticides. A key issue for the bioprocess design consists in adequately tracking a pre-specified optimal profile of the dissolved oxygen concentration. To this effect, this paper aims at developing a novel control law based on a nonlinear dynamic inversion method. The closed-loop strategy includes an observer based on a Bayesian Regression with Gaussian Process, which is used for on-line estimating the biomass present in the bioreactor. Unlike other approaches, the proposed controller leads to an improved response time with effective disturbance rejection properties, while simultaneously prevents undesired oscillations of the dissolved oxygen concentration. Simulation results based on available experimental data were used to show the effectiveness of the proposal.

1. Introduction

Bioprocesses control strategies are important for reducing production costs and increasing productivity while simultaneously maintaining the product quality. *Bacillus thuringiensis* (*Bt*) is an aerobic bacterium used for the production of δ-endotoxins; and the obtained bioinsecticide is of great interest and importance on account of its low environmental impact. Since *Bt* is an aerobic bacterium, the dissolved oxygen concentration (C_{DO}) in the culture medium is an important production variable. Inadequate levels of oxygen could inhibit or limit the microorganism growth. The control of biotechnological processes that include aerobics microorganisms normally involves the feed of high oxygen flow rates, in order to ensure an excess of the dissolved oxygen concentration with respect to its nominal value (Rocha-Valadez et al., 2007).

Dissolved oxygen as a nutrient is often a growth-limiting substrate. An agitator is used to improve the bioreactor productivity by minimizing spatial gradients of substrate and cell concentrations. The agitation speed is chosen to render a proper mixing while avoiding excessive shear forces that might cause cells rupture (Henson, 2006). Several articles have studied the effect of the dissolved oxygen in medium for various microorganism cultures. For example, the aeration and agitation rates as well as the type and size of the fermenter and its accessories directly affect the volumetric oxygen transfer coefficient in the production of exopolysaccharides from *Enterobacter cloacae* WD7 in (Bandaiphet and Prasertsan, 2006). For an *E. coli* fed-batch culture, (de Maré and Hagander, 2006) developed a continuous-time phenomenological model for the oxygen dynamics. In that work, some model parameters have been estimated off-line from empirical formulas while others were assumed to be known.

Most research articles on *Bt* processes suggest that C_{DO} must be kept above the minimal critical value for the microorganism growth. Data on critical oxygen concentration in *Bt* fermentations (Moraes et al., 1980) indicate that high levels of C_{DO} promote the formation of toxic compounds for *Bt*, inhibiting this way microbial growth and product formation (Onken and Liefke, 1989). On the other hand, a C_{DO} lower than the minimum critical value for the microorganisms produces the well-know "oxygen limitation" effect. Besides, high and low C_{DO} as well as oxygen fluctuations, can be detrimental for protein expression (Konz et al., 1998). For

* Corresponding author.
E-mail addresses: sromoli@unsj.edu.ar (S. Rómoli), amicarelli@inaut.unsj.edu.ar (A.N. Amicarelli), rortiz@unsj.edu.ar (O.A. Ortiz), gscaglia@unsj.edu.ar (G.J.E. Scaglia), fernando@inaut.unsj.edu.ar (F. di Sciascio).

http://dx.doi.org/10.1016/j.compchemeng.2016.05.017
0098-1354/

most microorganisms, the critical C_{DO} ranges between 0.1 mg L^{-1} and 1 mg L^{-1}. These values are relatively low when compared with the O_2 solubility in a diluted aqueous medium at 30 °C (around 7.5 mg L^{-1}). Therefore, an appropriate O_2 flow should continuously be fed into the bioreactor to approximately compensate for its consumption rate. This is a key factor that must be taken into account when designing bioreactors for aerobic microorganism culture.

In some fermentations, the C_{DO} can also be used for estimating the microorganisms concentration in the medium when the O_2 consumption is known (Amicarelli et al., 2014; di Sciascio and Amicarelli, 2008). In particular, the *Bt* life has two phases: a vegetative phase and a sporulated phase. In batch *Bt* fermentations, the oxygen concentration is critical during a large part of the microorganisms growth (the vegetative phase), but later the oxygen demand decreases during the sporulation phase. Some typical C_{DO} profiles are available for fed-batch fermentations (Li et al., 2009; Wu et al., 2002). Moreover, in (Ribbons, 1969) data regarding breathing and C_{DO} is also reported. Some experimental results have shown a significant effect of the agitation speed on the *Bt* production during the stationary phase (Wu et al., 2002).

For the *Bt* process it has been verified (Ghribi et al., 2007) that: (i) a high C_{DO} increases the cell density while reduces the δ-endotoxins synthesis; and (ii) a C_{DO} profile that maximizes the microorganism productivity is achieved by maintaining the reactor aeration near to 60% or 70% of oxygen saturation during the first 5–7 h of fermentation, while a 40% of oxygen saturation should be maintained at the sporulation phase, until the end of fermentation and regardless of the carbon source used as substrate (Ghribi et al., 2007). All these features allow, in principle, a large-scale production of proteins insecticides with low production costs.

Also for this bioprocess, (di Sciascio and Amicarelli, 2008) proposed a biomass estimator based on Bayesian Regression with Gaussian Process (Kocijan, 2016; Rasmussen, 2006). In this case, biomass concentration is considered a stochastic process i.e. an uncertain dynamic system perturbed by a process noise where its evolution for a particular fermentation is a realization of the stochastic process. This same estimator is considered again in this work but now integrated in closed loop with the new controller proposal. Since the *Bt* life span exhibits highly different dynamics along its vegetative growth and sporulation phases, then the time evolution of the biomass concentration resembles a non-stationary stochastic process.

Bayesian Regression with Gaussian Process is a non-parametric technique based on both, experimental data and qualitative knowledge of the bioprocess (di Sciascio and Amicarelli, 2008). The Bayesian non-parametric framework is flexible enough to represent a wide variety of bioprocess data. It makes possible interpreting the prior distribution, computing the posterior and full predictive distributions, as well as evaluating the mean predictions and the predictive uncertainties. The estimation algorithm consists of three parts. At first, we need to choose a particular form of the covariance function, then we obtain the posterior distribution of the Bayes' rules from the likelihood and prior distributions, and finally, we integrate all the information contained in the observed data. For simplicity the prior mean function was set to be zero, without loss of generality provided that a constant term is included in the covariance function (Kuß, 2006; Williams and Rasmussen, 1996). In this way, it is possible to analytically express the posterior distribution (see e.g. (Mardia and Marshall, 1984)). The hyper-parameters are the "parameters" of the likelihood and prior distributions. In contrast, hyper-parameters of the covariance function are unknown, and must be determined using the training data. The maximization of the posterior distribution is known as the maximum at posterior (MAP) approach, which is a Bayesian version of the maximum likelihood estimate. The MAP estimate was found by using the mentioned analytical expression of the posterior distribution in a gradient descent, or conjugate-gradient optimization technique, to calculate a local maximum of the posterior distribution. The number of hyper-parameters of the covariance function linearly increases with n, the dimension of the input space.

As stated in (Ali et al., 2015), the trend in the use of observers for chemical process has changed from single-based observer design to hybrid observers design. For instance, the combination of a reduced-order observer with a sliding mode observer. This is in spite that single-based observers, as for example Bayesian Estimators and asymptotic or exponential observers, will still be applicable in many applications involving chemical process systems.

In other previous work, the C_{DO} control in the *Bt* process has been solved by using a Lyapunov-based controller (Amicarelli et al., 2010). However, relatively poor performances were detected in several simulated cases for changes in the C_{DO} set point. Motivated by this, in the present work, a novel controller based on nonlinear dynamic inversion is designed to track an available optimal C_{DO} profile (Ghribi et al., 2007) for the *Bt* production process in order to improve the control system performance. The derived control law requires the biomass on-line knowledge, provided by the already mentioned biomass estimator. The proposed methodology is evaluated on the original *Bt* process model (Amicarelli et al., 2010) integrated with the biomass observer (di Sciascio and Amicarelli, 2008). All fermentation data considered corresponds to experiments that were carried out with glucose-based substrates (Amicarelli et al., 2010; Ghribi et al., 2007).

The paper is organized as follows. Section 2 describes the microorganism and the mathematical phenomenological model for the *Bt* process. The methodology for the controller design is presented in Section 3. Through several simulated experiments, Section 4 compares the performances of the new control law, the Lyapunov-based controller (Amicarelli et al., 2010), and a classical PID controller. Main conclusions and remarks are summarized in the last section.

2. Materials and methods

2.1. Microorganism and bioprocess characteristics

After the *Bt* vegetative growth, the beginning of the sporulation phase is induced by a substrate deficiency, called the mean exhaustion point. Normally the sporulation phase is accompanied by the production of crystal proteins known as δ-endotoxins. After sporulation, the process is completed with the cellular wall rupture (cellular lysis), and the subsequent liberation of spores and crystals to the culture medium (Aronson, 1993; Liu and Tzeng, 2000; Starzak and Bajpai, 1991).

In a previous work, several *Bt* fermentations experiments have been used for modeling and validating the bioprocess, and particularly the C_{DO} dynamics (Amicarelli et al., 2010; Atehortúa et al., 2007); and such conditions were adopted for the current work. The microorganisms were *Bacillus thuringiensis serovar. kurstaki* strain 172-0451, isolated and stored in the culture collection of the *Unidad de Biotecnología y Control Biológico* (Colombia) (Amicarelli et al., 2010). Growth experiments of the *Bt* fermentation process were performed in a reactor of 20 L of nominal volume, with an effective cultivation medium of 11 liters. The pH of the medium was adjusted to 7.0 with KOH before heat sterilization. Culture conditions at harvest are typified by 90% free spores and δ-endotoxins crystals. The temperature was kept around 30 °C by using an ON/OFF controller; whereas the pH was automatically controlled between 6.5 and 8.5 through a PID controller. The air flow and the agitation speed rate were set up at 22 L/min and 400 rpm, respec-

tively. Manometric pressure in the reactor was set at 41,368 Pa using a pressure controller. The readings of temperature, pH, and dissolved oxygen were registered by a data acquisition system (using an Advantech® PCL card). Biomass quantification was done with the dry weight method, i.e. dry cell weight (DCW) = (final weight – initial weight)/(volume of filtered microbial suspension) (Madigan et al., 1997). The glucose concentration was quantified with the reducing sugar method that uses the reagent Dinitrosalicilic Acid (Miller, 1959). The reagents concentration used for the pH control was nitric acid (5N) and potassium hydroxide (2N). The foam formation was avoided by aggregating a sterile antifoam solution manually.

The *Bt* δ-endotoxins production is an aerobic operation, i.e. the cells require oxygen as a substrate to achieve cell growth and product formation. The duration of the batch fermentation is limited and depends on the initial conditions of the microorganism culture. All the fermentations were initialized with the same inoculums and different substrate concentration conditions (Atehortúa et al., 2007). When the medium is inoculated, the biomass concentration increases at expense of reducing the nutrients. The fermentation concludes when the glucose that limits *Bt* growth is consumed, or when 90% or more of cellular lysis has occurred. Without considering the latency period (the bioprocess dead time is not considered in this study), the duration of each experiment varies between 14 h and 18 h, approximately. The model was developed in the works of (Atehortúa et al., 2007) and posteriorly (Amicarelli et al., 2010) added the dissolved oxygen dynamic.

The model equations are (see Table 1 for notation):

Vegetative cells balance:

$$\frac{dX_v(t)}{dt} = \underbrace{\mu X_v(t)}_{\text{Growth rate of vegetative cell}} - \underbrace{k_d X_v(t)}_{\text{death rate of vegetative cell}} - \underbrace{k_s X_v(t)}_{\text{sporulation rate of vegetative cell}}$$

$$\frac{dX_v(t)}{dt} = \underbrace{(\mu - k_d - k_s)}_{\mu_v} X_v(t) = \mu_v X_v(t). \quad (1)$$

where μ is the gross specific growth rate of vegetative cells, k_d is the relative death rate of vegetative cells, k_s is a kinetic constant representing the spore formation rate, and μ_v is the net specific growth rate of vegetative cells.

$$\mu_v = \mu - k_d - k_s \quad (2)$$

$$k_d^{(n)} = k_{d\max}\left(\frac{1}{1+e^{G_d(t_0+nT_0-P_d)}}\right) - k_{d\max}\left(\frac{1}{1+e^{G_d(t_0-P_d)}}\right) \quad (3)$$

$$k_s^{(n)} = k_{s\max}\left(\frac{1}{1+e^{G_s(S^{(n)}-P_s)}}\right) - k_{s\max}\left(\frac{1}{1+e^{G_s(S_0-P_s)}}\right) \quad (4)$$

Dissolved oxygen C_{DO} is considered a second limited growth substrate, therefore μ is modeled using a double Monod kinetic expression (Ryder and Sinclair, 1972).

$$\mu = \mu(S, C_{DO}) = \mu_{\max}\left(\frac{S(t)}{(K_S + S(t))}\frac{C_{DO}(t)}{(K_O + C_{DO}(t))}\right), \quad 0 \le \mu \le \mu_{\max} \quad (5)$$

Sporulated cells balance:

$$\frac{dX_s(t)}{dt} = k_s X_v(t) \quad (6)$$

Total cells balance ($X(t) = X_v(t) + X_s(t)$):

$$\frac{dX(t)}{dt} = \frac{dX_v(t)}{dt} + \frac{dX_s(t)}{dt} = (\mu - k_d)X_v(t)$$
$$= (\mu - k_d)\underbrace{\frac{X_v(t)}{X(t)}}_{f_v} X(t) = (\mu - k_d) f_v X(t) = \mu_X X(t) \quad (7)$$

where f_v is a fraction of vegetative cells, and μ_X is the net specific growth rate of total cells.

$$\mu_X = \frac{1}{X(t)}\frac{dX(t)}{dt} = \frac{d[\log X(t)]}{dt} = (\mu - k_d) f_v \quad (8)$$

Substrate concentration balance:

It is assumed that the vegetative cells are the only ones that consume substrate; therefore the evolution of substrate concentration $S(t)$ is given by the following differential equation:

$$\frac{dS(t)}{dt} = -q_S X_v(t). \quad (9)$$

where q_S is the net specific substrate uptake rate and is used to determine the biomass growth and the cell maintenance (the part of substrate consumption not used for growth purposes (Van Bodegom, 2007)).

$$q_S = -\frac{1}{X_v(t)}\frac{dS(t)}{dt} = -\frac{1}{X_v(t)}\underbrace{\frac{dX_v(t)}{dt}}_{\mu_v X_v(t)}\underbrace{\frac{dS(t)}{dX_v(t)}}_{1/Y_{X/S}} = \frac{\mu_v}{Y_{X/S}} = \frac{\mu_v}{Y_{X/S}^{\max}} + m_S. \quad (10)$$

where $Y_{X/S}$ is the observed, or apparent biomass growth yield on substrate, $Y_{X/S}^{\max}$ is theoretical or true biomass growth yield on substrate, and m_S is the substrate consumption coefficient for maintenance (Pirt, 1965). For increasing net specific growth rate μ_v, $Y_{X/S}$ and $Y_{X/S}^{\max}$ approach each other. The true growth yield $Y_{X/S}^{\max}$ is related to the observed yield coefficient $Y_{X/S}$ by:

$$\frac{1}{Y_{X/S}^{\max}} = \frac{1}{Y_{X/S}} - \frac{m_S}{\mu_v} \quad (11)$$

$$\frac{dS(t)}{dt} = -\left(\frac{\mu_v}{Y_{X/S}^{\max}} + m_S\right)X_v(t) = -\underbrace{\frac{\mu_v}{Y_{X/S}^{\max}}X_v(t)}_{\text{substrateconsumption forbiomass growth}} - \underbrace{m_S X_v(t)}_{\text{substrateconsumption forcellmaintenance}} \quad (12)$$

In order to analyze the validity of this model, it can be verified that the substrate consumption rate does not become negative, i.e.$q_S \ge 0$.

Taking into account that from Eqs. (3)–(5): $k_d \ge 0$, $k_s \ge 0$, $0 \le \mu \le \mu_{\max}$, and that by definition $Y_{X/S}^{\max} > 0$, $m_s \ge 0$.

$$q_S = \frac{\mu - k_d - k_s}{Y_{X/S}^{\max}} + m_S \ge 0 \quad \rightarrow \quad \mu \ge k_d + k_s - Y_{X/S}^{\max} m_S$$

Table 1
Variables in the model.

Symbol	Description
S	substrate concentration $\left[\text{g L}^{-1}\right]$
q_S	net specific substrate uptake rate $\left[\text{g substrate g cells}^{-1}\text{h}^{-1}\right]$
t	time [h]
X_s	sporulated cells concentration $\left[\text{g L}^{-1}\right]$
X_v	vegetative cells concentration $\left[\text{g L}^{-1}\right]$
X	total cell concentration $\left[\text{g L}^{-1}\right]$
C_{DO}	dissolved oxygen concentration $\left[\text{g L}^{-1}\right]$
μ	gross specific growth rate $\left[\text{h}^{-1}\right]$
μ_v	net specific growth rate $\left[\text{h}^{-1}\right]$
μ_X	net specific growth rate of total cells $\left[\text{h}^{-1}\right]$
$\mu_{\max}$	maximum specific growth rate $\left[\text{h}^{-1}\right]$
m_S	maintenance constant $\left[\text{g substrate g cells}^{-1}\text{h}^{-1}\right]$
k_s	kinetic constant representing the spore formation $\left[\text{h}^{-1}\right]$
k_d	death cell specific rate $\left[\text{h}^{-1}\right]$
$Y_{x/s}$	Observed biomass growth yield based on substrate consumed $\left[\text{g cells g substrate}^{-1}\right]$
$Y_{X/S}^{\max}$	Theoretical biomass growth yield based on substrate consumed $\left[\text{g cells g substrate}^{-1}\right]$
K_S	Substrate saturation constant $\left[\text{g substrate L}^{-1}\right]$
K_O	Oxygen saturation constant $\left[\text{g oxygen L}^{-1}\right]$
C_{sat}	oxygen saturation concentration (DOC concentration in equilibrium with the oxygen partial pressure of the gaseous phase) $\left[\text{g L}^{-1}\right]$
$k_{s\max}$	maximum kinetic constant $\left[\text{h}^{-1}\right]$
$k_{d\max}$	maximum death cell specific rate $\left[\text{h}^{-1}\right]$
Gs	gain constant of the sigmoid equation for spore formation rate $\left[\text{L g}^{-1}\right]$
Gd	gain constant of the sigmoid equation for death cell specific rate $\left[\text{h}^{-1}\right]$
Ps	position constant of the sigmoid equation for spore formation rate $\left[\text{g L}^{-1}\right]$
Pd	position constant of the sigmoid equation for death cell specific rate [h]
Y_{X/O_2}	Observed biomass growth yield based on oxygen consumed $\left[\text{g cells g oxygen}^{-1}\right]$
$Y_{X/O_2}^{\max}$	True Biomass growth yield based on oxygen consumed $\left[\text{g cells g oxygen}^{-1}\right]$
$\frac{1}{Y_{X/O_2}^{\max}}$	Oxygen consumption constant by growth [dimensionless] $\left[\text{g oxygen g cells}^{-1}\right]$
m_{O_2}	Oxygen consumption constant for maintenance $[\text{h}^{-1}]$ $\left[\text{g oxygen g cells}^{-1}\text{h}^{-1}\right]$
K_{air}	Ventilation constant $\left[\text{L}^{-1}\right]$
K_La	Volumetric oxygen mass transfer rate $\left[\text{h}^{-1}\right]$
q_{O_2}	Net specific oxygen uptake rate $\left[\text{g oxygen g cells}^{-1}\text{h}^{-1}\right]$
F_{air}	Inlet air flow rate that enters the bioreactor $\left[\text{Lh}^{-1}\right]$
OTR	Oxygen transfer rate $\left[\text{g oxygenL}^{-1}\text{h}^{-1}\right]$
OUR	Oxygen uptake rate $\left[\text{g oxygenL}^{-1}\text{h}^{-1}\right]$
S_0	Initial glucose concentration $\left[\text{g L}^{-1}\right]$
t_0	Initial fermentation time [h]

Therefore$q_S \geq 0$when $\mu(S, C_{DO}) \geq k_d + k_s - Y_{X/S}^{\max} m_S$. The minimum net specific substrate uptake rate $q_{S,\min} = \min(q_S)$is obtained when the substrate is exhausted ($\mu(S = 0,\ C_{DO} > 0) = 0$).

$$q_{s,\,\min} = m_s - \frac{(k_d + k_s)}{Y_{X/S}^{\max}} \tag{13}$$

$$\begin{cases} Y_{X/S}^{\max} = 0.37 \\ m_S = 0.005 \\ k_d = 0.1 \\ k_s = 0.5 \end{cases} \Rightarrow \quad q_{s,\,\min} = m_s - \frac{(k_d + k_s)}{Y_{X/S}^{\max}} = 0.005 - 1.621 < 0. \tag{14}$$

The inequality Eq. (14) shows that for *Bacillus thuringiensis*, $q_{S,\,\min}$ is negative, therefore Eq. (12) predicts that when $q_S = q_{S,\,\min}$ the substrate S increase i.e. act as an internal substrate source (Doran, 2013). This is an unrealistic feature of the model. From computational point of view, this undesirable problem can be avoided by considering only the positive solutions ($S(t) \geq 0$) of Eq. (9) when $q_S > 0(\mu \geq k_d + k_s - Y_{X/S}^{\max} m_S)$, that is:

$$S(t) = \underset{\substack{s(t)\,\geq\,0 \\ q_S\,\geq\,0}}{\text{sol}} \left\{ \frac{dS(t)}{dt} + q_S X_v(t) = 0 \right\} \Rightarrow \frac{dS(t)}{dt}$$

$$= \begin{cases} -q_S X_v(t) & ,\ \text{if} q_S \geq 0,\ \text{and}\ S(t) \geq 0 \\ 0 & ,\ \text{if} q_S < 0,\ \text{or}\ S(t) < 0 \end{cases} \tag{15}$$

Dissolved Oxygen Balance:
The standard model for dissolved oxygen balance is:

$$\frac{dC_{DO}(t)}{dt} = K_L a\,(C_{sat} - C_{DO}(t)) - q_{O_2} X(t) = OTR(t) - OUR(t). \tag{16}$$

where C_{DO} is the dissolved oxygen concentration, C_{sat} the oxygen saturation in equilibrium with the oxygen partial pressure of the

gaseous phase, $K_L a$ is the volumetric oxygen mass transfer rate, and q_{O_2} is the net specific oxygen uptake rate. The first term in the second member is the rate of aeration or OTR (oxygen transfer rate from air bubble to liquid phase), and the second term is the rate of oxygen consumption by cells or OUR (oxygen uptake rate of cells per volume of broth).

The aeration term (OTR) can be written as follows (Amicarelli et al., 2010):

$$OTR(t) = K_{air} F_{air} (C_{sat} - C_{DO}(t)) \tag{17}$$

where K_{air} is an oxygen consumption parameter by growth (constant for each fermentation), and F_{air} is the inlet air flow rate that enters the bioreactor. For a given bioreactor configuration, F_{air} is mainly a function of the impeller agitation speed.

Based on experimental evidence (Atehortúa et al., 2007), it is assumed that the oxygen consumption rate (OUR) depends on the total cells X, that is, both vegetative and sporulated cells consume oxygen at different rates, therefore:

$$\mathrm{OUR}(t) = q_{O_2} X(t) \tag{18}$$

Because dissolved oxygen is considered as a second substrate q_{O_2} is of similar form to that q_S, then:

$$q_{O_2} = \frac{\mu_X}{Y_{X/O_2}} = \frac{\mu_X}{Y^{\max}_{X/O_2}} + m_{O_2}. \tag{19}$$

where Y_{X/O_2} is the observed biomass yield based on oxygen consumed, $Y^{\max}_{X/O_2}$ is the true biomass yield based on oxygen used for growth, and m_{O_2} is the oxygen consumption coefficient for respiration maintenance.

$$\mathrm{OUR}(t) = q_{O_2} X(t) = \underbrace{\frac{\mu_X}{Y^{\max}_{X/O_2}} \mathrm{X(t)}}_{\substack{O_2 \text{ consumption} \\ \text{forbiomass growth}}} + \underbrace{m_{O_2} \mathrm{X(t)}}_{\substack{O_2 \text{ consumption} \\ \text{forcellmaintenance}}} \tag{20}$$

Replacing in (20) $\mu_X X(t) = (\mu - k_d) X_v(t)$, and $X(t) = X_v(t) + X_s(t)$, we obtain:

$$OUR(t) = \left[\frac{\mu - k_d}{Y^{\max}_{X/O_2}} + m_{O_2} \right] X_v(t) + m_{O_2} X_s(t) = q^v_{O_2} X_v(t) + q^s_{O_2} X_s(t) \tag{21}$$

$$q^v_{O_2} = \frac{\mu - k_d}{Y^{\max}_{X/O_2}} + m_{O_2}, \quad q^s_{O_2} = m_{O_2}.$$

where $q^v_{O_2}$, and $q^s_{O_2}$ are the specific oxygen uptake rate for vegetative and sporulated cells respectively. Eq. (21) shows explicitly that both vegetative and sporulated cells consume oxygen at different rates. This is the model of oxygen uptake rate proposed by Park et al. (p. 1023, Eq. (A.9)), (Park et al., 2009) for endospore-forming bacteria (such as *Bacillus thuringiensis*).

As we did before with the substrate consumption model, we now analyze if the net specific oxygen uptake rate q_{O_2} does become negative.

Taking into account that $0 \le \mu \le \mu_{\max}$, $k_d \ge 0$, $Y^{\max}_{X/O_2} > 0$, $f_v \ge 0$, and $m_{O_2} \ge 0$. Comparing Eqs. (20) and (21) it is obvious that $q_{O_2} \ge 0$ if always $q^v_{O_2} \ge 0$ because $q^s_{O_2} = m_{O_2}$ is positive. Then, we analyze if $q^v_{O_2}$ does become negative.

$$q^v_{O_2} = \frac{\mu - k_d}{Y^{\max}_{X/O_2}} + m_{O_2} \ge 0 \;\rightarrow\; k_d - Y^{\max}_{X/O_2} m_{O_2} \le \mu$$

For *Bacillus thuringiensis* $q^v_{O_2}$ is positive because the inequality $0 \le k_d - Y^{\max}_{X/O_2} m_{O_2} \le \mu \le \mu_{\max}$ always holds, therefore q_{O_2} is also positive.

$$\begin{cases} Y^{\max}_{X/O_2} = 263.15 \\ m_{O_2} = 0.00073 \\ k_d = 0.1 \end{cases} \Rightarrow \quad \mu \ge \underbrace{k_d}_{0.1} \underbrace{- Y^{\max}_{X/O_2} m_{O_2}}_{0.192} = -0.092$$

Alternatively, by replacing Eq. (7) ($\mu_X X(t) = dX(t)/dt$) in Eq. (20), we obtain an equivalent model of oxygen uptake rate:

$$\mathrm{OUR(t)} = \frac{1}{Y^{\max}_{X/O_2}} \frac{dX(t)}{dt} + m_{O_2} X(t) \tag{22}$$

This form of implementation of the oxygen consumption model has been widely reported in the literature; see the review by Garcia-Ochoa et al., 2010, p. 296, Eq. (14) (Garcia-Ochoa et al., 2010), and references therein. This model form has also been specifically applied to modeling *Bacillus thuringiensis* oxygen uptake rate (Amicarelli et al., 2010; Ollis, 1983; Rowe et al., 2003).

The oxygen uptake rate models Eqs. (20)–(22) are mathematically equivalent. The model Eq. (21) was significantly more explanatory power than model Eq. (22), but from a computational point of view, the last one is better than the others. This is so, because the time-discretized model Eq. (23) is a linear difference equation with constant coefficients.

$$\begin{aligned} \mathrm{OUR(t)} &= \frac{1}{Y^{\max}_{X/O_2}} \frac{dX(t)}{dt} + m_{O_2} X(t) \underset{T_0}{\rightarrow} OUR^{(n)} \\ &= \left[\frac{1}{Y^{\max}_{X/O_2} T_0} + m_{O_2} \right] X^{(n)} - \frac{1}{Y^{\max}_{X/O_2} T_0} X^{(n-1)} \end{aligned} \tag{23}$$

Consequently, we decided to adopt the following model for Dissolved Oxygen Balance:

$$\frac{dC_{DO}(t)}{dt} = K_{air} F_{air} (C_{sat} - C_{DO}(t)) - \frac{1}{Y^{\max}_{X/O_2}} \frac{dX(t)}{dt} - m_{O_2} X(t) \tag{24}$$

This model differs from reported models, by including dynamics for natural death of cells and substrate consumption for cell maintenance. It uses sigmoid functions to describe these kinetic parameters (Eqs. (3) and (4)).

In the work of (Atehortúa et al., 2007) two model were developed: a batch model and a fed-batch model. Both of them were made with experimental data of batch fermentations. For the fed-batch modeling balance, terms associated with flow streams of reactor and tangential filter were added in order to represent fed-batch operation characteristics. The hypothesis in the work of Atehortúa was that the IFBC-TCR can be modeled using parameters estimated from experimental data of batch cultures. With this intention, a fed-batch model was developed and validated using experimental data from four batch cultures with different initial glucose concentrations (8, 21, 32 and 40 g/L). During the validation of the model for IFBC-TCR process, the need of four different sets of model parameters in accordance with operation region. Following the stated hypothesis, initial glucose concentration values for batch cultures were chosen among values of glucose concentration reached during typical IFBC-TCR (8–40 g/L). Then, the four sets of parameters for batch model were identified and validated by considering that each batch model covers a region of intermittent fed-batch culture operation (see Table 2). A single commutation among the four batch parameter sets will provide valid parameters for IFBC-TCR model during its time evolution. Maximum glucose concentration in the medium (S_{max}) was used as the switching criteria among the estimated batch parameter sets. Such modeling

Table 2
Set of model parameters for batch and for the intermittent fed-batch culture with total cell retention of *Bacillus thuringiensis subsp. Kurstaki*.

	$S_{max} \leq 10$g/L	10g/L $< S_{max} \leq$ g/L	20g/L $< S_{max} <$ 32g/L	$S_{max} \geq 32$g/L
μ_{max}	0.8	0.7	0.65	0.58
$Y_{X/S}$	0.7	0.58	0.37	0.5
K_s	0.5	2	3	4
K_O	1.5×10^{-3}	1.5×10^{-3}	1.5×10^{-3}	1.5×10^{-3}
m_s	0.005	0.005	0.005	0.005
ks max	0.5	0.5	0.5	0.5
Gs	1	1	1	1
Ps	1	1	1	1
$k_{d\,max}$	0.1	0.1	0.1	0.1
Gd	5	5	5	5
Pd	4	4.7	4.9	6
$\frac{1}{Y^{max}_{X/O_2}}$	9.725×10^{-4}	4.502×10^{-3}	3.795×10^{-3}	1.597×10^{-3}
m_{O_2}	1.589×10^{-4}	8.14×10^{-4}	0.729×10^{-3}	5.61×10^{-4}
K_{air}	4.636×10^{-4}	3.369×10^{-4}	2.114×10^{-3}	1.045×10^{-3}
C_{sat}	0.00745	0.00745	0.00745	0.00745

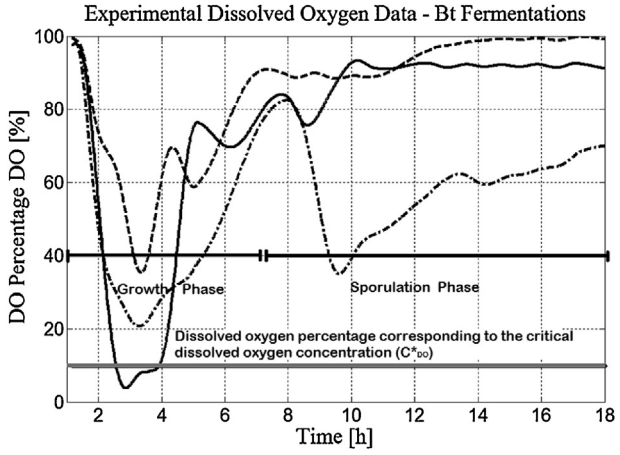

Fig. 1. Example of experimental results of dissolved oxygen concentration for some typical batch fermentations from (Amicarelli et al., 2010).

approach is called subspace modeling, and replies gain scheduling technique of control theory (Bequette, 2003). In this work the objective is the control of dissolved oxygen in the batch process. However, the batch operation can be originate from any of the initial conditions mentioned above (8, 21, 32 and 40 g/L). Table 2 presents the sets of parameters according to the initial condition employed.

According to experimental results obtained for the δ-endotoxins production of *Bt*, in some cases one can observe that the C_{DO} decreases to values lower than the critical one (10%) (Atehortúa et al., 2007), even when it is assumed that air flow rate is in excess. Fig. 1 presents experimental results of three fermentations under the same operations conditions. In Fig. 1, two important facts can be seen: first, the critical influence of the oxygen along a large fraction of the microorganism growth (the vegetative phase); and second, the notorious fall in the C_{DO} demand during the sporulation phase. This situation occurs on most fermentations and the limitations caused by oxygen have been detected under various operating conditions. In the particular case of Fig. 1, the air flow rate was set at 22 L/min, which is assumed to ensure an oxygen excess, or at least to ensure a C_{DO} higher than the critical C_{DO} reported for the microorganism (10% of the saturation concentration). The C_{DO} in the culture medium decays along the first fermentation hours (first 5–7 h from a total of 18 h for completing the process). In some cases, the C_{DO} can decay even below its critical value (e.g. in one of the 3 fermentations presented in Fig. 1). In contrast, the oxygen demand decreases when the sporulation starts (after around the first 8 h). These results suggest that a C_{DO} control strategy is necessary for optimizing the *Bt* process.

3. Controller design

One issue of capital importance in bioprocess is the capability of maintain bounded in a desired interval some important variables. More precisely, in some bioprocess is desirable to make the system follow pre-established profiles of the principal variables. These "optimal" profiles are the best policy to operate a process because they ensure lower production costs, higher productivities, better product quality, and/or make the process more environmentally friendly. As it is stated before, in the *Bt* process the C_{DO} was determined to be a critical variable for maximizing the δ–endotoxins production. This is due, principally, to the importance of the oxygen concentration in the vegetative phase of the microorganism growth and to the remarkable fall in the dissolved oxygen demand on the sporulation phase. The latest is an essential point because, in this type of bioprocess, there is not air outlet, so the air should be fed in such a way that an oxygen inhibition could not be probable (Rocha-Valadez et al., 2007). As we have pointed out previously, the inlet air flow rate F_{air} depends of the agitation speed. Consequently, in order to control the dissolved oxygen concentration we will use the air flow as the manipulated variable by way of varying the impeller speed.

Below is presented the methodology based on inverse dynamics used for designing a controller for the profile tracking of the oxygen given by (Ghribi et al., 2007), assumed to be an optimal feeding policy (Kamoun et al., 2009).

3.1. Controller design

The control action required to follow the state variable profiles showed in (Ghribi et al., 2007) is calculated based on the previously described process model. To this effect, the discrete version the continuous bioprocess model can be written through the forward Euler approximation as:

$$\begin{cases} X_v^{(n+1)} = [1 + T_0(\mu^{(n)} - k_d^{(n)} - k_s^{(n)})]X_v^{(n)} & (a) \\ X^{(n+1)} = X^{(n)} + T_0[\mu^{(n)} - k_d^{(n)}]X_v^{(n)} & (b) \\ S^{(n+1)} = S^{(n)} - T_0\left[\dfrac{\mu^{(n)} - k_d^{(n)} - k_s^{(n)}}{Y^{max}_{X/S}} + m_S\right]X_v^{(n)} & (c) \\ C_{DO}^{(n+1)} = C_{DO}^{(n)} + T_0 K_{air} F_{air}^{(n)}(C_{sat} - C_{DO}^{(n)}) - \left(\dfrac{1}{Y^{max}_{X/O_2}} + T_0 m_{O_2}\right)X^{(n)} + \dfrac{1}{Y^{max}_{X/O_2}}X^{(n-1)} & (d) \\ \mu^{(n)} = \mu_{max}\left(\dfrac{S^{(n)}}{K_S + S^{(n)}}\dfrac{C_{DO}^{(n)}}{K_O + C_{DO}^{(n)}}\right) & (e) \\ k_d^{(n)} = k_{d_{max}}\left(\dfrac{1}{1 + e^{G_d(t_0 + nT_0 - P_d)}}\right) - k_{d_{max}}\left(\dfrac{1}{1 + e^{G_d(t_0 - P_d)}}\right) & (f) \\ k_s^{(n)} = k_{s_{max}}\left(\dfrac{1}{1 + e^{G_S(S^{(n)} - P_S)}}\right) - k_{s_{max}}\left(\dfrac{1}{1 + e^{G_S(S_0 - P_S)}}\right) & (g) \end{cases} \quad (25)$$

where T_0 is the sampling time (within this paper it is adopted as 0.1 *h*, selected by using a Fourier frequency analysis (di Sciascio and Amicarelli, 2008)).

Consider first, the immediately reachable value of the dissolved oxygen concentration, as proposed here:

$$C_{DO}^{(n+1)} = C_{DO_{ref}}^{(n+1)} - K_{DO}(C_{DO_{ref}}^{(n)} - C_{DO}^{(n)}) \quad (26)$$

where the subscript "ref" refers to the optimal dissolved oxygen reference profile (Ghribi et al., 2007), and K_{DO} is a controller parameter. This replacement force the system to evolve from the actual state ($C_{DO}^{(n)}$) to the reference one ($C_{DO_{ref}}^{(n+1)}$) in the next sampling time. Thus,

the dissolved oxygen concentration tends gradually to the reference, forcing the whole bioprocess to follow the desired reference profile.

In Eq. (26), the controller parameter fulfils $0 < K_{DO} < 1$ making the tracking errors tend to zero when $n \to \infty$ (this is proved below). Then, the value of the dissolved oxygen in the next sampling time is a function of the reference profile $C_{DO_{ref}}^{(n+1)}$and $C_{DO_{ref}}^{(n)}$ the actual state variable ($C_{DO}^{(n)}$) and the controller parameter (K_{DO}).

Remark. Observe in Eq. (26) that:

If $K_{DO} = 0$, the reference trajectory is reached in only one step, then the control actions will be very violent. This probably leads to the undesirable consequences, for example: saturation of the actuators, excessive foam generation, or excessive shear forces that might cause cells rupture.

If $0 < K_{DO} < 1$, the system will effortlessly reach the optimal reference profile.□

Operating on (25.d), we obtain the expression of the control command$F_{air}^{(n)}$.

$$F_{air}^{(n)} = \frac{1}{T_0 K_{air}(C_{sat} - C_{DO}^{(n)})}\left[\left(C_{DO}^{(n+1)} - C_{DO}^{(n)}\right) + \left(\frac{1}{Y_{X/O_2}^{max}} + m_{O_2}\right)X^{(n)} - \frac{1}{Y_{X/O_2}^{max}}X^{(n-1)}\right] \quad (27)$$

Now, note that, in the current sampling time, $C_{DO}^{(n+1)}$is unknown. However, it can be replaced by Eq. (26). This leads to the following control law:

$$F_{air}^{(n)} = \frac{1}{T_0 K_{air}\left(C_{sat} - C_{DO}^{(n)}\right)}\left[C_{DO_{ref}}^{(n+1)} - K_{DO}\left(C_{DO_{ref}}^{(n)} - C_{DO}^{(n)}\right) - C_{DO}^{(n)} + \left(\frac{1}{Y_{X/O_2}^{max}} + m_{O_2}\right)X^{(n)} - \frac{1}{Y_{X/O_2}^{max}}X^{(n-1)}\right] \quad (28)$$

If the control action is calculated with Eq. (28) and is replaced in (25.d), we obtain Eq. (26).

3.2. Asymptotic convergence to zero of the tracking error

The difference between the reference and the real profile is called tracking error, and is given by:

$$e^{(n)} = C_{DO_{ref}}^{(n)} - C_{DO}^{(n)} \quad (29)$$

In what follows, we prove that the proposed controller guarantee asymptotic convergence to zero of the tracking error.

Operating mathematically with Eq. (26),

$$C_{DO_{ref}}^{(n+1)} - C_{DO}^{(n+1)} = K_{DO}(C_{DO_{ref}}^{(n)} - C_{DO}^{(n)}) \quad (30)$$

Then, the tracking error is calculated as Eq. (29) for two sampling times

$$e^{(n+1)} = C_{DO_{ref}}^{(n+1)} - C_{DO}^{(n+1)}$$
$$e^{(n)} = C_{DO_{ref}}^{(n)} - C_{DO}^{(n)} \quad (31)$$

Replacing Eqs. (31) in (30) leads to

$$e^{(n)} = K_{DO}e^{(n-1)} = (K_{DO})^2 e^{(n-2)} = \cdots = (K_{DO})^n e^{(0)} \quad , \quad |e^{(0)}| < \infty \quad (32)$$

if $0 < K_{DO} < 1$ (obviously the initial error is bounded)

$$\lim_{n\to\infty} e^{(n)} = 0 \quad (33)$$

Hence, Eq. (32) tends to zero when $0 < K_{DO} < 1$ and $n \to \infty$, thus showing that the tracking errors tend to zero, $e^{(n)} \to 0$, $n \to \infty$.

3.3. Selection of optimal controller parameters

In the field of systems and control, probabilistic methods have been found useful especially for problems related to robustness of uncertain systems (Tempo and Ishii, 2007). One of these methods, the Monte Carlo Randomized Algorithm, is widely used in many fields such as the diffusing spins, to calculate parameter likelihood, the estimation of parameters uncertainty, and to perform singular spectrum analysis (Albrecht, 2013; Hall and Alexander, 2009; Jemwa and Aldrich, 2006; Müller et al., 2014). In the control area, Monte Carlo methods allow to estimate an expectation value and they provide effective tools for the probabilistic analysis of robustness of control schemes. In this subsection, the Monte Carlo method is applied to select an optimal controller parameter.

The complete application of this method is explained elsewhere (Tempo and Ishii, 2007). In this paper, it is used Eq. (8) of the above mentioned paper with a confidence value (δ) of 0.01, and an accuracy of 0.007 (ε). Then, it is necessary to make 1000 simulations. The method is developed as follows: (i) N random values of the parameter is selected; (ii) a cost function that evaluates the controller performance is defined; and (iii) the optimal parameters are determined by means of an optimization procedure.

The performance function, namely cost function, is equal to the cumulative squared error, which can be numerically approximated as follows:

$$C = T_0\frac{(C_{DO_{ref}} - C_{DO})^2}{2} \quad (34)$$

Although the optimum is not guaranteed, the Monte Carlo Experiment provides an approximate solution based on a large number of trials (N). Hence, 1000 values of each parameter ranging from 0 to1 were simulated. This parameter range ensures convergence to zero of the tracking error (see Section 3.2). The lowest cost is obtained in simulation number 122, where the parameter value was: $K_{DO} = 0.0015$.

4. Comparison with a Lyapunov based controller

In this section, the effectiveness of the proposed control law in closed loop with the Bayesian observer (di Sciascio and Amicarelli, 2008) is verified through simulation examples. This section demonstrate, through several examples, that the proposed control law based on inverse dynamics has a better performance than the Lyapunov based controller, designed in (Amicarelli et al., 2010).

The principal objective of the control scheme in the *Bt* δ-endotoxins production is to follow a reference profile of the dissolved oxygen. The foremost challenge of the chosen reference profile is the step at the sixth hour of operation.

So as to compare the Lyapunov controller with the inverse dynamics based controller, five tests are implemented. In this paper, the proposed controller is similarly tested to (Amicarelli et al., 2010) so that the comparison between them is direct. In the first test, the controller performance under normal operating conditions is shown. Secondly, a perturbation in the control action is included. In third place, the system is disturbed with a step change. Then, a 20% of biomass estimation error and a 10% model parametric errors are included. Finally, a One-Sided Monte Carlo Randomized Algorithm is applied in order to verify the performance of the proposed controller under a 20% model parameter uncertainty.

In addition, with the purpose of compare the proposed controller with another controller of the literature, it is shown the comparison of the performance between the inverse dynamics based controller and a PID controller, designed in (Amicarelli et al., 2008).

4.1. Normal operation conditions

The controller performance is tested when the process is operated under normal conditions. The model parameters are detailed in Table 2. The optimal controller parameter obtained in the previous section is used. Fig. 2a shows the tracking of the reference profile without undesirable oscillations, compared with the Lyapunov based controller. To better reveal the performance of the control law the tracking error (see Eq. (29)) is shown in Fig. 2b.

It can be observed from the figures that the inverse dynamics based controller is able to accurately maintain the C_{DO} in the set point with reduced rise time compared with the Lyapunov controller. This demonstrates the ability of the inverse dynamics controller not only to assess large and small changes in the reference profile but its quick response in adjusting the airflow rate.

After the step at the sixth hour of operation, the Lyapunov based controller has two undesired negative peaks in the dissolved oxygen concentration. Besides this peak represents a 125% lower concentration compared with the reference value, the dissolved oxygen concentration remains in a lower value than the critical one. This means that the microorganism suffer a lack of oxygen for a while, leading to a certain death of the vegetative cell. Since the primary purpose of this process is to maximize the sporulated cells concentration, the undesired peak performed when a Lyapunov controller is used, is completely unacceptable.

In conclusion, the Lyapunov controller fails to respond as quickly and as accurately as the proposed controller does. Moreover, the designed controller shows improvements in response time and in avoiding oscillations.

Now, compared with the PID controller, the effectiveness of the proposed controller is easy to appreciate in Fig. 3. Fig. 3a shows the tracking of the reference profile without undesirable oscillations and with an improved response time, compared with the PID controller. To disclose better the performance of the control law, the tracking error Eq. (29) is shown in Fig. 3b. The control of processes that have long dead time, oscillatory output and unstable sub-process, such as biochemical plants, require a higher-level architecture controller than one degree-of-freedom PID controller tuned by one set of three parameters (Alford, 2006; Maghade and Patre, 2012). Nevertheless, this type of controllers are difficult to design compare with the methodology based on inverse dynamics presented in this paper.

Fig. 4 shows the comparison between the control actions of the three controllers. As it was expected, the control actions are quite similar. Due to the low value of K_{DO}, the inverse dynamics controller tends to saturate the control action in the first hours of operation.

4.2. Perturbation in the control action

So as to demonstrate the controller performance, a random perturbation in the control action is included, as is suggested in (Vega et al., 2014). In this paper, a random perturbation using MATLAB® is employed: the control action is modified with a 20% of its value. The function used was "*random (norm, 0, 0.2)*", which is a random noise normally distributed with zero mean and a standard deviation of 0.2 (George, 2014). From Eq. (28), the control action is calculated and then, the perturbation is added:

$$F_{air_{\text{perturbed}}}^{(n-1)} = F_{air_{\text{unperturbed}}}^{(n-1)} \times (random('norm', 0, 0.2) + 1) \quad (35)$$

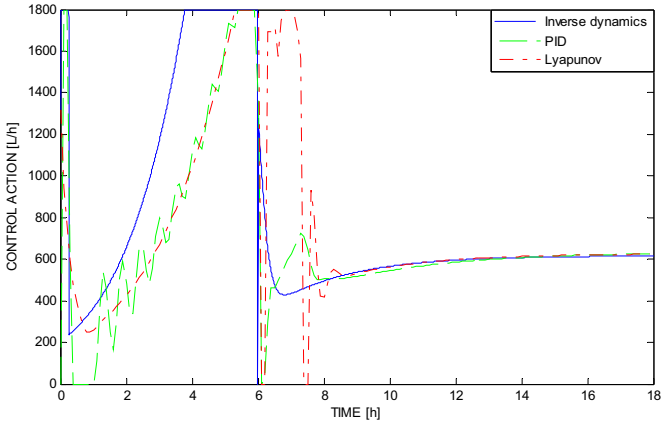

Fig. 4. Control actions of each controller.

The following figures illustrate the previously described results. The control action calculated compared with the feed flow rate in normal operation conditions is shown in Fig. 5a, and the controller performance is evaluated through the tracking error (Fig. 5b).

As shown in Fig. 5b, when a Gaussian disturbance is introduced, the tracking error increases. Nevertheless, the tracking error is still low and bounded compared with those obtained by other authors in the literature (Amicarelli et al., 2010, 2008).

4.3. Step disturbance in the feed flow rate

As (Lübbert and Bay Jørgensen, 2001) state, although a rich theory has been developed for the robust control of linear systems, there is a slight knowledge about the robust control of nonlinear systems with constraints, like most bioprocesses. Control systems maintaining stability when the system's dynamics (parameter uncertainty, error in the state variables estimation, fluctuation in the control action) deviates slightly, are said to be robust. Then, one way to ensure the stability consists on introducing a step-change perturbation in the control action and evaluate the performance of the controller under this perturbation. As proposed in (Tebbani et al., 2008), a feed flow rate 40% higher than calculated is adopted. In (Craven et al., 2014) the authors discuss the existence of non-modeled disturbances faced during the real-time implementation of a bioprocess. It is not possible predict disturbances in bioprocess due to its inherent complexity and its strongly coupled variables. So, in this paper is introduced a step-change perturbation in the control action throughout the batch time.

Fig. 6a compares the feed flow rate of the proposed controller normal operation (named Control action in the normal operation) and the calculated control action under the step disturbance (named Control action of the disturbed system). Fig. 6b shows that the tracking error obtained with the proposed controller when the system dynamics deviates from its normal condition, remains similar to the normal operation, thus providing a test of robustness.

4.4. Biomass estimation and model parametric errors

In general, between several batch fermentations there exist unavoidable differences in process conditions and therefore the task of modeling is normally complicated. The bioprocess always presents strong nonlinearity, disturbance presence from the external environment (foreign microorganism, alterations in the substrate feeding), and even when the process conditions are the same in all fermentations, the microorganisms can behave dif-

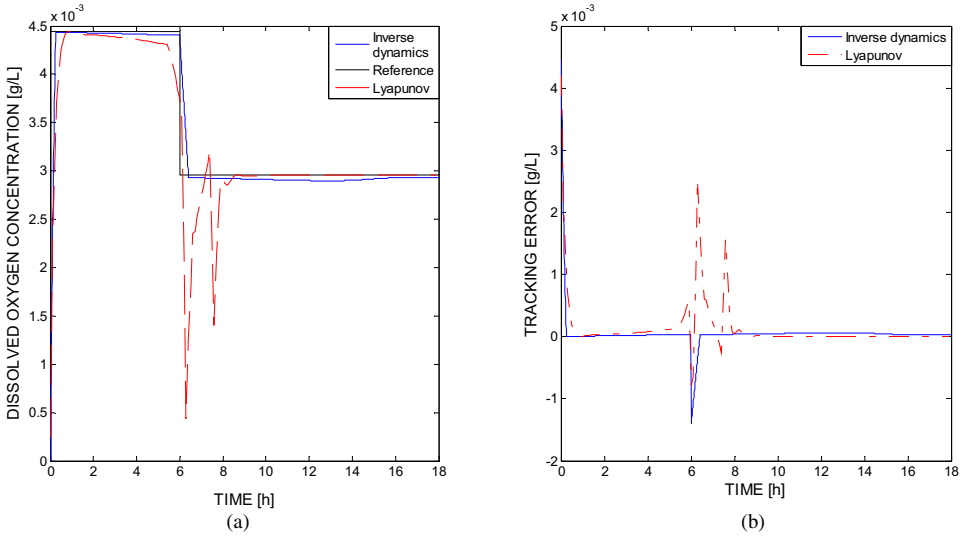

Fig. 2. (a) Dissolved oxygen concentration: it is shown the results with the linear algebra based controller, the Lyapunov based controller and the reference profile. (b) Comparison between the tracking errors (Eq. (29)) of the Lyapunov controller and the inverse dynamics controller.

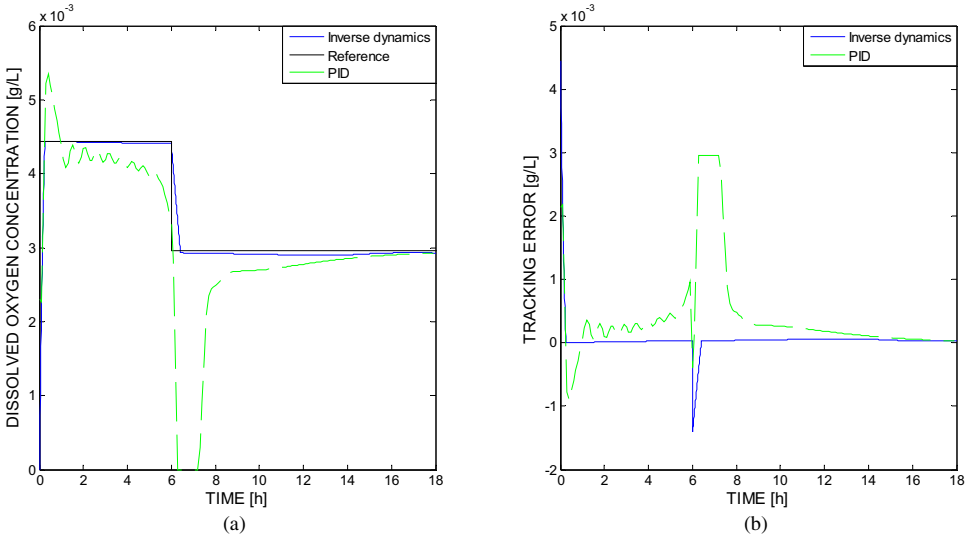

Fig. 3. (a) Comparison of the performance between the proposed controller and the PID controller. (b) Comparison of the tracking errors between the proposed controller and the PID controller.

ferently every time. In (Amicarelli et al., 2010) it was adopted a first principles model that represents functional (causal) relations between physical variables, succeeding in understanding the bioprocess evolution. The experimental data used in the parameters identification were sufficiently representative of a set of available batch fermentations, and the parameters probability density distributions obtained are consistent with the experimental data record lengths. However, due to the above mentioned, it is necessary to test the designed controller when there are errors in the state variables estimation and in the model parameters.

Fig. 7a shows an example of the performance of the designed dissolved oxygen controller in closed-loop with a biomass estimator, most specifically shows the controller output for 20% biomass estimation errors and for 10% model parametric errors compared with the Lyapunov based controller. In Fig. 7b the tracking error is shown for both cases (with and without estimation and parametric model errors). The inverse dynamics based controller succeeds in following the reference C_{DO} profile despite the existence of errors in the biomass estimation and in the model parameters.

4.5. Performance of the controller under parameter uncertainty

In this subsection, a Monte Carlo simulation is performed to demonstrate the effectiveness of the controller from a statistical viewpoint (Hao et al., 2014; Michail et al., 2014; Ricardez-Sandoval, 2012), under parameter uncertainty. In order to prove the robustness of the controller designed, some parameters described in Tables 1 and 2 are varied in a range of ±20% of its nominal values. Within the Monte Carlo Randomized Algorithms, this is an example of the worst-case problem.

In this experiment is adopted a confidence value (δ) of 0.01 and an accuracy (ε) of 0.007. Then, it is necessary to make 1000 simulations.

Fig. 8a shows the C_{DO} for the 1000 simulations. This figure shows clearly that the performance of the controller is stable, because the state variable tends to the reference profile without undesirable oscillations, although there are a 20% of uncertainly in the bioreactor parameters.

Fig. 8b depicts the performance function, defined in Eq. (34), for 1000 sets of the system parameters. It is shown that the tracking

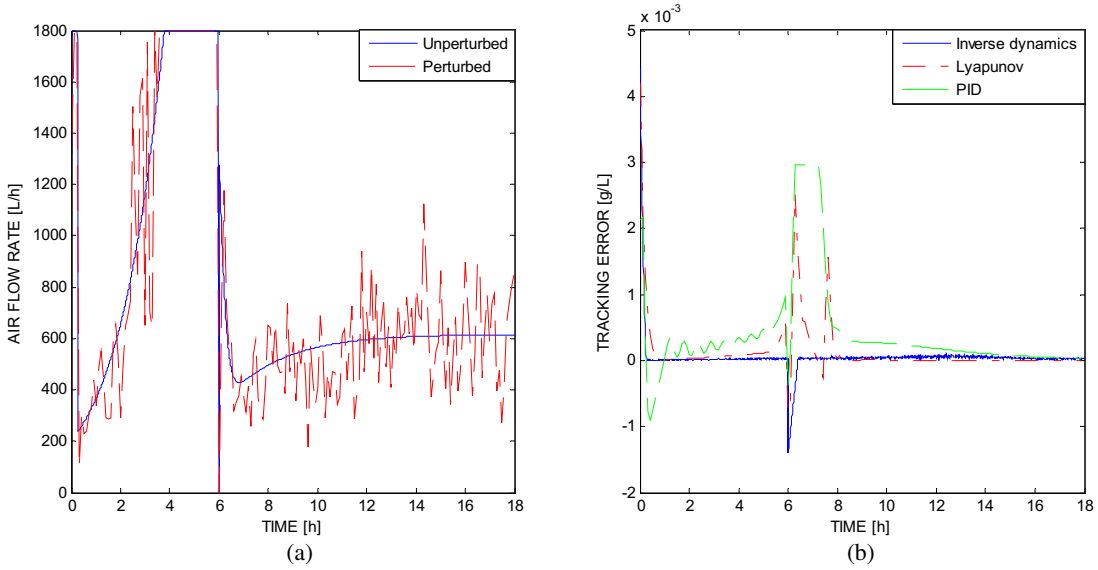

Fig. 5. (a) Control action of the proposed controller with aleatory noise compared with the controller without noise. (b) Tracking errors of the proposed controller with noise compared with the Lyapunov controller and the PID controller.

errors, reflected in the performance function C, remain bounded. Then, it follows that if 1000 simulations with different values randomly chosen of all the parameters are carried out, and the tracking errors remains bounded, there is a 99% probability that the performance of the controller will be proper whatever the parameter values are in a range of ±20%.

5. Conclusions

A new control law for tracking an optimal concentration profile in a batch bioreactor has been presented. The proposed method allows to control a nonlinear system.

A One-Sided Monte Carlo Randomized Algorithm is used in order to find the controller parameter that minimizes the tracking error. The controller performance has been compared with others one-step ahead controllers (i.e. myopic controllers), a Lyapunov controller proposed in (Amicarelli et al., 2010) and a PID controller proposed in (Amicarelli et al., 2008). This paper has demonstrated that they fail to respond quickly and accurately compared to the controller designed in this paper. This controller shows improvement in response time, oscillations and disturbance rejection. Monte Carlo simulation results are provided to demonstrate the effectiveness of the controller in the presence of parameter uncertainty.

In general, such methodology can be applied to many nonlinear systems, making it a promising technique for its application to several processes of the biochemical industry. Besides, the present methodology has the advantage of using discrete equations, and therefore a direct implementation in most computer-driven systems is feasible. Results of the implementation indicated the response of the controller was satisfactory in real time, which confirmed the applicability of inverse dynamics for controller implementation and the feasibility of the overall design to run a bioreactor process autonomously. Finally a few words about a future work: a Model Predictive Control (MPC) strategy of dissolved oxygen is developed in a work done by us and submitted for publication in a control journal.

The MPC improve the performance of the dissolved oxygen control for this process compared with a classic PID, PI control, with controller based in Lyapunov theory and with the controller presented in this work. The behavior of the MPC in the change of the reference profile is most adequate because never achieve the

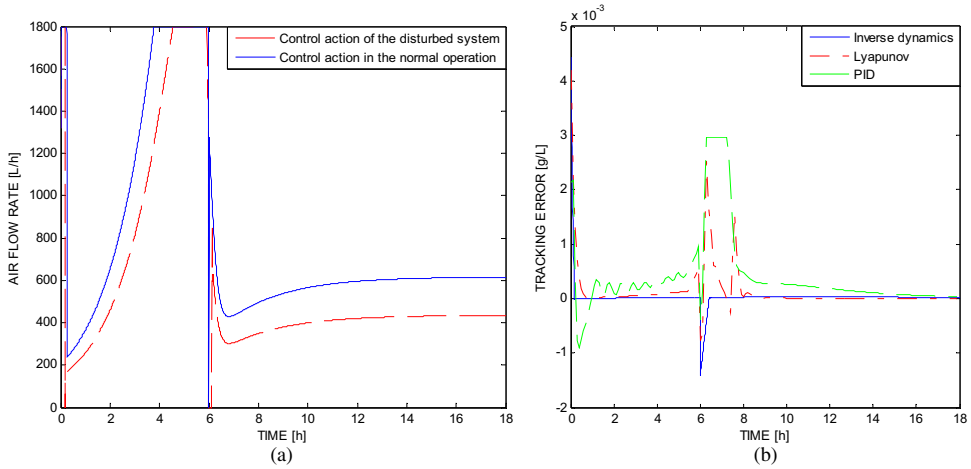

Fig. 6. (a) Comparison between the systems perturbed with a step in all the batch time with the unperturbed system. (b) Comparison of the tracking errors between the proposed controller with a step disturbance and the other two controllers without disturbance.

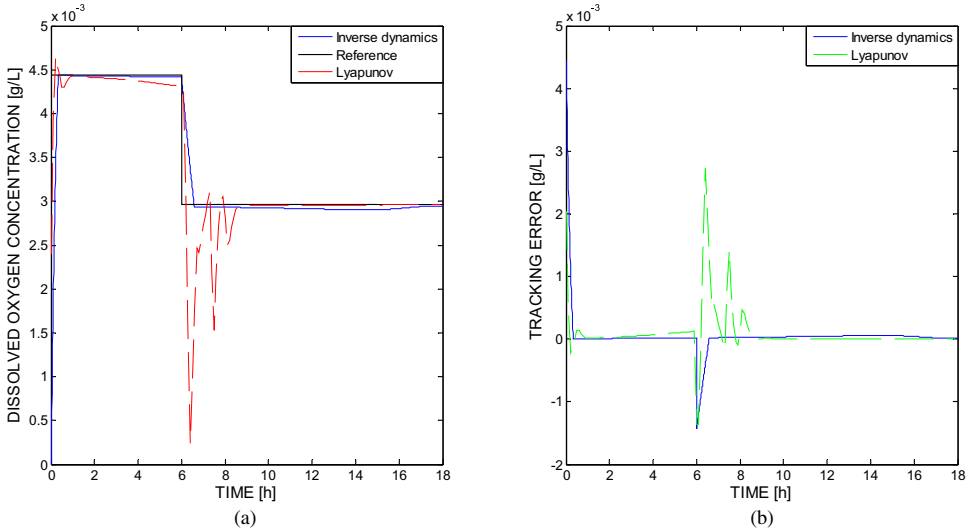

Fig. 7. (a) Dissolved oxygen concentration with a 20% of biomass estimation error and 10% of model parameters errors of the proposed controller compared with the Lyapunov controller. (b) Tracking errors with a 20% of biomass estimation error and 10% of model parameters errors of the proposed controller compared with the Lyapunov controller.

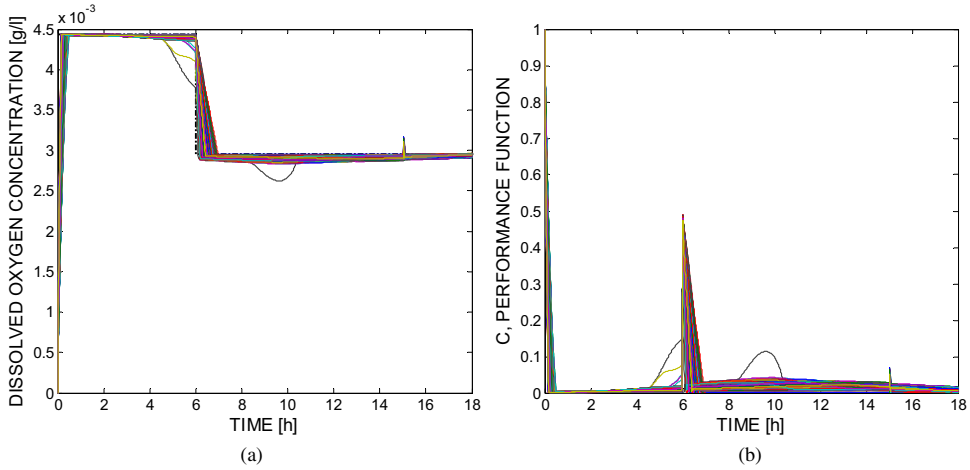

Fig. 8. (a) Dissolved oxygen concentration for 1000 sets of the system parameters, m_s, k_{smax}, Ps, Gs, k_{emax}, Ge, Pe, μ_{max}, $Y_{X/S}$, K_s, K_d, K_1, K_2, K_3 and C_{sat} of the Monte Carlo Experiment. (b) Performance function *C* for 1000 sets of the system parameters of the Monte Carlo Experiment.

critical value that can cause microorganism inhibition also, performance indexes IAE and ITAE are lower for the MPC. These results are expected, because the performance of myopic controllers are not comparable with controllers with prediction capabilities as Model Predictive Controllers (i.e. N-step ahead controllers, N > 1).

Acknowledgements

This work was partially funded by National Council of Scientific and Technological Research (CONICET) and Universidad Nacional de San Juan (UNSJ).

References

Albrecht, J., 2013. Estimating reaction model parameter uncertainty with Markov Chain Monte Carlo. Comput. Chem. Eng. 48, 14–28.
Alford, J.S., 2006. Bioprocess control: advances and challenges. Comput. Chem. Eng. 30, 1464–1475.
Ali, J.M., Hoang, N.H., Hussain, M.A., Dochain, D., 2015. Review and classification of recent observers applied in chemical process systems. Comput. Chem. Eng. 76, 27–41.
Amicarelli, A., Toibero, J., Quintero, O., di Sciascio, F., Carelli, R., 2008. Control de oxígeno disuelto para fermentación batch de bt. In: Semana Del Control Automático XXI Congreso Argentino De Control Automático, Buenos Aires, Argentina.
Amicarelli, A., di Sciascio, F., Toibero, J., Alvarez, H., 2010. Including dissolved oxygen dynamics into the Bt δ-endotoxins production process model and its application to process control. Braz. J. Chem. Eng. 27, 41–62.
Amicarelli, A., Quintero, O., Sciascio, F., 2014. Behavior comparison for biomass observers in batch processes. Asia-Pac. J. Chem. Eng. 9, 81–92.
Aronson, A.I., 1993. The two faces of Bacillus thuringiensis: insecticidal proteins and post-exponential survival. Mol. Microbiol. 7, 489–496.
Atehortúa, P., Álvarez, H., Orduz, S., 2007. Modeling of growth and sporulation of Bacillus thuringiensis in an intermittent fed batch culture with total cell retention. Bioprocess Biosyst. Eng. 30, 447–456.
Bandaiphet, C., Prasertsan, P., 2006. Effect of aeration and agitation rates and scale-up on oxygen transfer coefficient, k L a in exopolysaccharide production from Enterobacter cloacae WD7. Carbohydr. Polym. 66, 216–228.
Bequette, B.W., 2003. Process Control: Modeling, Design, and Simulation. Prentice Hall PTR.
Craven, S., Whelan, J., Glennon, B., 2014. Glucose concentration control of a fed-batch mammalian cell bioprocess using a nonlinear model predictive controller. J. Process Control 24, 344–357.
de Maré, L., Hagander, P., 2006. Parameter estimation of a model describing the oxygen dynamics in a fed-batch E. coli cultivation. Biotechnol. Lett. 27, 983–990.
di Sciascio, F., Amicarelli, A.N., 2008. Biomass estimation in batch biotechnological processes by Bayesian Gaussian process regression. Comput. Chem. Eng. 32, 3264–3273.
Doran, P.M., 2013. Bioprocess Engineering Principles. Academic Press, Waltham MA.
Garcia-Ochoa, F., Gomez, E., Santos, V.E., Merchuk, J.C., 2010. Oxygen uptake rate in microbial processes: an overview. Biochem. Eng. J. 49, 289–307.

George, J., 2014. On adaptive loop transfer recovery using Kalman filter-based disturbance accommodating control. IET Control Theory Appl. 8, 267–276.
Ghribi, D., Zouari, N., Trabelsi, H., Jaoua, S., 2007. Improvement of Bacillus thuringiensis delta-endotoxin production by overcome of carbon catabolite repression through adequate control of aeration. Enzyme Microb. Technol. 40, 614–622.
Hall, M.G., Alexander, D.C., 2009. Convergence and parameter choice for Monte-Carlo simulations of diffusion MRI. IEEE Trans. Med. Imaging 28, 1354–1364.
Hao, H., Zhang, K., Ding, S.X., Chen, Z., Lei, Y., 2014. A data-driven multiplicative fault diagnosis approach for automation processes. ISA Trans. 53, 1436–1445.
Henson, M.A., 2006. Biochemical reactor modeling and control. IEEE Control Syst. 26, 54–62.
Jemwa, G.T., Aldrich, C., 2006. Classification of process dynamics with Monte Carlo singular spectrum analysis. Comput. Chem. Eng. 30, 816–831.
Kamoun, F., Zouari, N., Saadaoui, I., Jaoua, S., 2009. Improvement of Bacillus thuringiensis bacteriocin production through culture conditions optimization. Prep. Biochem. Biotechnol. 39, 400–412.
Kocijan, J., 2016. Modelling and Control of Dynamic Systems Using Gaussian Process Models. Springer.
Konz, J.O., King, J., Cooney, C.L., 1998. Effects of oxygen on recombinant protein expression. Biotechnol. Progr. 14, 393–409.
Kuß, M., 2006. Gaussian Process Models for Robust Regression, Classification, and Reinforcement Learning.
Lübbert, A., Bay Jørgensen, S., 2001. Bioreactor performance: a more scientific approach for practice. J. Biotechnol. 85, 187–212.
Li, X., van der Steen, G., van Dedem, G., van der Wielen, L., van Leeuwen, M., van Gulik, W., Heijnen, J., Ottens, M., Krommenhoek, E., Gardeniers, J., 2009. Application of direct fluid flow oscillations to improve mixing in microbioreactors. AIChE J. 55, 2725–2736.
Liu, B.L., Tzeng, Y.M., 2000. Characterization study of the sporulation kinetics of Bacillus thuringiensis. Biotechnol. Bioeng. 68, 11–17.
Müller, D., Esche, E., López, C.D.C., Wozny, G., 2014. An algorithm for the identification and estimation of relevant parameters for optimization under uncertainty. Comput. Chem. Eng. 71, 94–103.
Madigan, M.T., Martinko, J.M., Parker, J., 1997. Brock biology of microorganisms.
Maghade, D.K., Patre, B.M., 2012. Decentralized PI/PID controllers based on gain and phase margin specifications for TITO processes. ISA Trans. 51, 550–558.
Mardia, K.V., Marshall, R.J., 1984. Maximum likelihood estimation of models for residual covariance in spatial regression. Biometrika 71, 135–146.
Michail, K., Zolotas, A.C., Goodall, R.M., 2014. Optimised sensor selection for control and fault tolerance of electromagnetic suspension systems: a robust loop shaping approach. ISA Trans. 53, 97–109.
Miller, G.L., 1959. Use of dinitrosalicylic acid reagent for determination of reducing sugar. Anal. Chem. 31, 426–428.
Moraes, I., Santana, M., Hokka, C., 1980. The influence of oxygen concentration on microbial insecticide production. London, Canada In: Adv. Biotechnol., Proceedings of 6th International Fermentation Symposium, Vol. 1, pp. 75–79.
Ollis, D.F., 1983. A simple batch fermentation model: theme and variations. Ann. N. Y. Acad. Sci. 413, 144–156.
Onken, U., Liefke, E., 1989. Effect of total and partial pressure (oxygen and carbon dioxide) on aerobic microbial processes. In: Bioprocesses and Engineering. Springer, pp. 137–169.
Park, S., Rittmann, B.E., Bae, W., 2009. Life-cycle kinetic model for endospore-forming bacteria, including germination and sporulation. Biotechnol. Bioeng. 104, 1012–1024.
Pirt, S., 1965. The maintenance energy of bacteria in growing cultures. Proc. R. Soc. Lond. B: Biol. Sci. 163, 224–231.
Rasmussen, C.E., 2006. Gaussian processes for machine learning.
Ribbons, D.W., 1969. Automatic assessment of respiration during growth in stirred fermentors. Appl. Microbiol. 18, 438–443.
Ricardez-Sandoval, L.A., 2012. Optimal design and control of dynamic systems under uncertainty: a probabilistic approach. Comput. Chem. Eng. 43, 91–107.
Rocha-Valadez, J.A., Albiter, V., Caro, M.A., Serrano-Carreón, L., Galindo, E., 2007. A fermentation system designed to independently evaluate mixing and/or oxygen tension effects in microbial processes: development, application and performance. Bioprocess Biosyst. Eng. 30, 115–122.
Rowe, G.E., Margaritis, A., Wei, N., 2003. Specific oxygen uptake rate variations during batch fermentation of Bacillus thuringiensis subspecies kurstaki HD-1. Biotechnol. Progr. 19, 1439–1443.
Ryder, D., Sinclair, C., 1972. Model for the growth of aerobic microorganisms under oxygen limiting conditions. Biotechnol. Bioeng. 14, 787–798.
Starzak, M., Bajpai, R.K., 1991. A structured model for vegetative growth and sporulation in Bacillus thuringiensis. Appl. Biochem. Biotechnol. 28, 699–718.
Tebbani, S., Dumur, D., Hafidi, G., 2008. Open-loop optimization and trajectory tracking of a fed-batch bioreactor. Chem. Eng. Process.: Process Intensif. 47, 1933–1941.
Tempo, R., Ishii, H., 2007. Monte Carlo and Las Vegas randomized algorithms for systems and control: an introduction. Eur. J. Control 13, 189–203.
Van Bodegom, P., 2007. Microbial maintenance: a critical review on its quantification. Microb. Ecol. 53, 513–523.
Vega, P., Lamanna de Rocco, R., Revollar, S., Francisco, M., 2014. Integrated design and control of chemical processes—part I: revision and classification. Comput. Chem. Eng. 71, 602–617.
Williams, C.K., Rasmussen, C.E., 1996. Gaussian processes for regression.
Wu, W.-T., Hsu, Y.-L., Ko, Y.-F., Yao, L.-L., 2002. Effect of shear stress on cultivation of Bacillus thuringiensis for thuringiensin production. Appl. Microbiol. Biotechnol. 58, 175–177.